# Synthesis, Crystal Structure, and Magnetic Properties of Oxalato−Copper(II) Complexes with 3,3-Bis(2-imidazolyl)propionic Acid, an Imidazole−Carboxylate Polyfunctional Ligand: From Mononuclear Entities to Ladder-Like Chains

**Y. Akhriff,[†] J. Server-Carrió,[†] A. Sancho,[†] J. García-Lozano,[†] E. Escrivá,[†] J. V. Folgado,[‡] and L. Soto*,[†]**

Departament de Química Inorgànica, Universitat de València, c/Vicent Andrés Estellés, s/n, 46100 Burjassot (València), Spain, and ICMUV, Universitat de València, c/Dr. Moliner 50, 46100 Burjassot (València), Spain

*Received August 13, 1998*

The synthesis of five new Cu(II) compounds of formula $[Cu(HBIP)(C_2O_4)]\cdot H_2O$ (**1**), $[Cu(HBIP)(C_2O_4)(OH_2)]\cdot 2H_2O$ (**2**), $[\{Cu(HBIP)Cl\}_2(\mu\text{-}C_2O_4)]\cdot 2H_2O$ (**3**), $[\{Cu(BIP)\}_2(\mu\text{-}C_2O_4)]\cdot 2H_2O$ (**4**) and $[\{Cu(BIP)\}_2(\mu\text{-}C_2O_4)]\cdot 6H_2O$ (**5**), together with their spectral and magnetic characterization, is reported. Crystal structures of compounds **2**, **3** and **5** have been solved. All these compounds crystallize in the triclinic system, space group $P\bar{1}$, with $a = 7.3322(3)$ Å, $b = 10.014(1)$ Å, $c = 11.541(1)$ Å, $\alpha = 113.22(1)°$, $\beta = 91.37(1)°$, $\gamma = 94.51(1)°$, $Z = 2$ for compound **2**; $a = 7.444(2)$ Å, $b = 8.518(2)$ Å, $c = 11.231(2)$ Å, $\alpha = 97.45(2)°$, $\beta = 98.99(2)°$, $\gamma = 97.95(2)°$, $Z = 1$ for compound **3**; and $a = 7.977(1)$ Å, $b = 8.656(1)$ Å, $c = 11.807(1)$ Å, $\alpha = 69.06(1)°$, $\beta = 86.07(1)°$, $\gamma = 67.36(1)°$, $Z = 1$ for compound **5**. In compound **2** the asymmetric unit consists of one isolated neutral $[Cu(HBIP)(C_2O_4)(OH_2)]$ molecule and two noncoordinated water molecules. The Cu(II) ion is five-coordinated (4+1 coordination mode) with HBIP and oxalato entities acting as bidentate ligands and the water molecule as the fifth ligand. The structure of compound **3** is made up of centrosymmetric binuclear $[\{Cu(HBIP)(Cl)\}_2(\mu\text{-}C_2O_4)]$ units and noncoordinated water molecules. The two copper atoms are linked through a bis-bidentate oxalato group leading to a metal−metal separation of 5.28(3) Å. The coordination stereochemistry of the $CuN_2O_2Cl$ chromophore is approximately SP. Compound **5** exhibits a structure built of ladder-like chains. In these chains the rungs are constituted by the neutral dinuclear centrosymmetric $[(BIP)Cu(C_2O_4)Cu(BIP)]$ entities. The oxalato group bridges two copper atoms in a bis-bidentate fashion, whereas the BIP acts as a tridentate ligand, connecting through their carboxylate groups these dimeric units along the *a* axis. The copper atom is involved in a five-coordinated $CuN_2O_2O'$ chromophore, with a coordination geometry intermediate between SP and TBP. The magnetic properties of all complexes have been investigated. Compound **1** and **2** follow a Curie−Weiss law with very low values of $\theta$. The other three compounds exhibit an antiferromagnetic coupling, with $2J = -265$ cm$^{-1}$ for **3**, $2J = -108$ cm$^{-1}$ for **4**, and $2J = -5.7$ cm$^{-1}$ for **5**. The strength of the exchange interaction is discussed on the basis of the structural features and correlated with published magneto-structural data on similar oxalato-bridged copper(II) compounds.

## Introduction

Polynuclear metal complexes are of considerable current interest in relation to the nature of magnetic exchange interactions between metal ions through bridging ligands[1−4] and as models for the active sites of metalloenzymes.[5−8] Many of these compounds are prepared in attempts to mimic the behavior of various dicopper proteins such as hemocyanin, tyrosinase, etc.[9−12] The active sites of these proteins usually involve copper coordinated to at least two nitrogen donor atoms coming from imidazole of histidine residues. In the Cu−Zn superoxide dismutase the copper ions are coordinated to three imidazoles and one imidazolate ($Im^-$) group acts as a bridging ligand between the two metals.[13,14] However it is of interest to note that the structure and chemical composition of the surrounding active site in the metalloproteins, namely, the hydrogen bond network, can also modulate their function.[15] Thus, the hydrogen

[†] Departament de Química Inorgànica.
[‡] ICMUV.

(1) Willet, R. D., Gatteschi, D., Kahn, O., Eds. *Magneto-Structural Correlations in Exchange Coupled Systems*; NATO ASI Series C 140; D. Reidel: Dordrecht, The Netherlands, 1985.
(2) Vicente, R.; Escuer, A.; Solans, X.; Font-Bardia, M. *J. Chem. Soc., Dalton Trans.* **1996**, 1835.
(3) Gatteschi, D., Kahn, O., Miller, J. S., Palacio, F., Eds. *Magnetic Molecular Materials*; Kluwer Academic Publishers: Dordrecht, The Netherlands, 1991.
(4) Kahn, O. *Molecular Magnetism*; VCH: New York, 1993.
(5) Bertini, I., Gray, H. B., Lippard, S. J., Valentine, J. S., Eds. *Bioinorganic Chemistry*; University Science Books: Mill Valley, CA, 1994.
(6) Lippard, S. J.; Berg, J. M. *Principles of Bioinorganic Chemistry*; University Science Books: Mill Valley, CA, 1994.
(7) Karlin, K. D.; Tyeklar, Z. *Bioinorganic Chemistry of Copper*; Chapman & Hall: New York, 1993.
(8) Holm, R. H.; Kennepohl, P.; Solomon, E. I. *Chem. Rev.* **1996**, *96*, 2239.
(9) Solomon, E. I.; Sundaram, U. M.; Machonkin, T. E. *Chem. Rev.* **1996**, *96*, 2563.
(10) Kitajima, N.; Moro-oka, Y. *Chem. Rev.* **1994**, *94*, 737.
(11) Karlin, K. D.; Tyeklár, Z. *Adv. Inorg. Biochem.* **1994**, *9*, 123.
(12) Karlin, K. D. *Science* **1993**, *261*, 701.
(13) Tainer, J. A.; Getzoff, E. D.; Richardson, J. S.; Richardson, D. C. *Nature* **1983**, *306*, 284.
(14) Bertini, I.; Banci, L.; Luchinat, C.; Piccioli, M. *Coord. Chem. Rev.* **1990**, *100*, 67.
(15) Christianson, D. W.; Alexander, R. S. *J. Am. Chem. Soc.*, **1989**, *111*, 6412.

10.1021/ic980982x CCC: $18.00 
Published on Web 02/25/1999

bonding between the imidazole moieties and neighboring carboxylate oxygen of the adjacent amino acid residue may orient the ligands for optimal metal coordination and may also enhance the electrostatic interaction between the metal ion and its ligands. Recent studies on the relationship between the function of enzymes and hydrogen bonding demonstrated that the activity is increased by hydrogen bonding, while it is highly decreased upon hydrogen bonding removal.[16−18] Thus, we believe that it could be particularly useful to include the imidazole and carboxylate moieties in a chelating ligand to provide low-molecular weight model copper(II) complexes. To our knowledge only a few such copper complexes have been characterized,[19,20] probably owed to the synthetic difficulties of incorporating the imidazole and carboxylate groups in a chelate ligand and because the complexes are difficult to obtain in a highly crystalline form and in most cases only insoluble powder samples were obtained. These difficulties have been overcome by different authors using other nitrogen donors, specially nitrogen-containing heterocyclic derivatives of no bioinorganic interest, such as pyridine, pyrazole, etc. It should be noted however that these ligands differ from imidazole in size and chemical properties; these facts have prompted the synthesis of polyimidazole ligands.[21−26] As a contribution to this field and as a part of our structural and chemical research on metal-imidazole-carboxylate systems we are focusing on the use of the ligand: 3,3-bis(2-imidazolyl)propionic acid, (designated hereafter HBIP). HBIP, containing two imidazole rings and carboxylate functionalities in the side chain, is a versatile ligand in the formation of metal complexes. Thus, in acidic or weakly alkaline media it might bind to a metal either through two N(imidazole) atoms and the carboxylate group, or may not use all its coordination possibilities depending on the coordination ability of a second ligand.[27] It is well-known the coordination capacity of the carboxylate groups, which may attach one or several metal atoms.[28,29] Thus, HBIP might play several roles as polidentate ligand when the carboxylate group is involved in the coordination. Under basic conditions, in addition the imidazole moiety offers the possibility of coordinating a second metal, through the other nitrogen of the imidazolate ($Im^-$) nucleus, to yield imidazolato-bridged complexes. Protonation or deprotonation at different sites such as ring imidazole and/or carboxylate groups may occur, depending upon such factors as pH of crystallization, charge neutralization requirements, etc. HBIP has recently been used by us to obtain a tetraimidazole derivative, [Cu(HBIP)(BIP)($ONO_2$)],[27] whose structural characterization shows that the two ligands are not equivalent, one of the acid groups keeping its hydrogen atom and the second one being deprotonated. Our interest in this area focuses on designing synthetic pathways for systems of variable dimensionality building from [HBIP-M-X] and/or [HBIP-M-X-M-HBIP] units, where M can be any metal of bioinorganic interest and X an extended-bridging ligand as carboxylate, imidazolate or oxalato. We report here the structural and/or spectroscopic characterization of five HBIP-containing copper(II) oxalato derivatives. In this system, the coordinating behavior of the oxalato group (bidentate or bis-bidentate) and the HBIP (bidentate or tridentate) depends on the experimental conditions, such as pH of crystallization and molar ratios. Moreover, the magnetic characterization of the studied compounds has permitted to explore the existence of magneto-structural correlations.

## Experimental Section

**Materials.** 3,3-Bis(2-imidazolyl)propionic acid (HBIP) was prepared according to Joseph et al.,[30] and characterized by $^1H$ NMR, $^{13}C$ NMR, and IR spectroscopy and powder X-ray diffraction. All other reagents were used as supplied. Elemental analyses (C, H, N, Cl) were performed by Servei de Microanalisi, Consell Superior d'Investigacions Cientifiques, Barcelona, Spain.

**[Cu(HBIP)($C_2O_4$)]·$H_2O$ (1) and [Cu(HBIP)($C_2O_4$)($OH_2$)]·$2H_2O$ (2).** Aqueuos solutions of HBIP (0.5 mmol, 30 mL) and $H_2C_2O_4$ (0.5 mmol, 5 mL) were mixed together. Addition of the resulting solution to an aqueous solution of $CuCl_2·2H_2O$ (0.5 mmol, 5 mL) immediately yielded a blue powder precipitate; the final pH value was 1.8. This precipitate was separated by filtration, washed with water and ethanol, and dried to constant weight at 70 °C yielding a violet powder, which corresponds to compound **1**. The filtrate was allowed to stand at room temperature for about 1 day to produce single blue crystals of complex **2**. The resulting crystals were separated by filtration and washed with water and ethanol. Anal. Calcd for $C_{11}H_{12}N_4O_7Cu$ (**1**): C, 35.13; H, 3.19; N, 14.90; Cu, 16.91. Found: C, 34.96; H, 3.08; N, 14.50; Cu, 16.98. Anal. Calcd for $C_{11}H_{16}N_4O_9Cu$ (**2**): C, 32.06; H, 3.89; N, 13.60; Cu, 15.43. Found: C, 31.96, H, 3.80; N, 13.50; Cu, 15.38.

**[{Cu(HBIP)Cl}$_2$($\mu$-$C_2O_4$)]·$2H_2O$ (3).** Aqueous solutions of HBIP (0.5 mmol, 40 mL) and of $H_2C_2O_4$ (0.25 mmol, 2.5 mL) were added to an aqueous solution (15 mL) of $CuCl_2·2H_2O$ (0.5 mmol) and NaCl (1 mmol); the final pH value was 1.8. The green powder which appeared was separated by filtration and washed with water and ethanol. Elemental analysis fits the formulation given for **3**. The remaining solution was allowed to stand at room temperature for about 3 days to produce the complex **3** as green crystals. The resulting crystals were separated by filtration and washed with water and ethanol. Anal. Calcd for $C_{20}H_{24}N_8O_{10}Cl_2Cu_2$ (**3**): C, 32.68; H, 3.27; N, 15.25; Cl, 9.65; Cu, 17.31. Found: C, 32.76, H, 3.31; N, 15.29; Cl, 9.71; Cu, 17.40.

**[{Cu(BIP)}$_2$($\mu$-$C_2O_4$)]·$2H_2O$ (4) and [{Cu(BIP)}$_2$($\mu$-$C_2O_4$)]·$6H_2O$ (5).** Aqueous solutions of $K_2C_2O_4$ (0.25 mmol, 2.5 mL) and $CuCl_2·2H_2O$ (0.5 mmol, 5 mL) were added to an alkaline solution of the ligand (0.5 mmol of HBIP and 1 mmol of KOH, 50 mL), giving a final pH of 6.8. The green powder which appeared corresponding to compound **4** was separated by filtration, washed with water and ethanol, and dried to constant weight at 70 °C. The remaining solution was allowed to stand at room temperature for about 3 weeks, yielding green prismatic crystals of compound **5**, which were separated by filtration and washed with water and ethanol. Anal. Calcd for $C_{20}H_{22}N_8O_{10}Cu_2$ (**4**): C, 36.28; H, 3.33; N, 16.93; Cu, 19.21. Found: C, 36.36; H, 3.28; N, 16.85; Cu, 19.35. Anal. Calcd for $C_{20}H_{30}N_8O_{14}Cu_2$ (**5**): C, 32.72; H, 4.09; N, 15.27; Cu, 17.33. Found: C, 32.96; H, 3.98; N, 15.50; Cu, 17.40.

Compounds **1**, **2**, and **4** can be also syntethized by interconversion reactions according to the following procedures.

**Compounds 1 and 2.** To an aqueous suspension of compound **3** or **4** (0.05 mmol, 40 mL) a solution of $H_2C_2O_4$ (0.025 mmol, 2.5 mL)

(16) Chen X.-M.; Ye, B.-H.; Huang X.-C.; Xu, Z.-T. *J. Chem. Soc*., *Dalton Trans.* **1996**, 3465.
(17) Lesburg, C. A.; Christianson, D. W. *J. Am. Chem. Soc*. **1995**, *117*, 6838.
(18) Kiefer, L. L.; Paterno, S. A.; Fierke, C. A. *J. Am. Chem. Soc*. **1995**, *117*, 6831.
(19) Tang, C. C.; Davalian, D.; Huang, P.; Breslow, R. *J. Am. Chem. Soc*. **1978**, *100*, 3918.
(20) Várnagy, K.; Sóvágó, I.; Ágoston, K.; Likó, Z.; Süli-Vargha, H.; Sanna, D.; Micera, G. *J. Chem. Soc*., *Dalton Trans.* **1994**, 2939.
(21) Dominguez-Vera, J. M.; Galvez, N.; Colacio, E.; Cuesta, R.; Costes, J.-P.; Laurent, J.-P. *J. Chem. Soc., Dalton Trans.* **1996**, 861.
(22) Bhalla, R.; Helliwell, M.; Garner, C. D. *Inorg. Chem.* **1997**, *36*, 2944.
(23) Likó, Z.; Süli-Vargha, H. *Tetrahedron Lett.* **1993**, *34*, 1673.
(24) Kodera, M.; Terasako, N.; Kita, T.; Tachi, Y.; Kano, K.; Yamazaki, M.; Koikawa, M.; Tokii, T. *Inorg. Chem.* **1997**, *36*, 3861.
(25) Lynch, W. E.; Kurtz, D. M.; Wang, S.; Scott, R. A. *J. Am. Chem. Soc*. **1994**, *116*, 11030.
(26) Tabbi, G.; Driessen, W. L.; Reedijk, J.; Bonomo, R. P.; Veldman, N.; Spek, A. L. *Inorg. Chem.* **1997**, *36*, 1168.
(27) Sancho, A.; Gimeno, B.; Amigó, J. M.; Ochando, L. E.; Debaerdemaeker, T.; Folgado, J. V.; Soto L. *Inorg. Chim. Acta* **1996**, *248*, 153.
(28) Porai-Koshits, M. A. *Zh. Strukt. Khim*. **1980**, *21*, 146.
(29) Agterberg, F. P. W.; Provó Kluit, H. A. J.; Driessen, W. L.; Oevering, H.; Buijs, W.; Lakin, M. T.; Spek, A. L.; Reedijk, J. *Inorg. Chem.* **1997**, *36*, 4321.
(30) Joseph, M.; Leigt, T.; Swain, M. L. *Synthesis* **1977**, 459.

**Table 1.** Crystallographic Data for $[Cu(HBIP)(C_2O_4)(OH_2)]\cdot 2H_2O$ (**2**), $[\{Cu(HBIP)Cl\}_2(\mu\text{-}C_2O_4)]\cdot 2H_2O$ (**3**), and $[\{Cu(BIP)\}_2(\mu\text{-}C_2O_4)]\cdot 6H_2O$ (**5**)

| | **2** | **3** | **5** |
|---|---|---|---|
| formula | $C_{11}H_{16}N_4O_9Cu$ | $C_{20}H_{24}N_8O_{10}Cl_2Cu_2$ | $C_{20}H_{30}N_8O_{14}Cu_2$ |
| fw | 411.8 | 734.5 | 733.6 |
| space group (No.) | $P\bar{1}$ (2) | $P\bar{1}$ (2) | $P\bar{1}$ (2) |
| *a*, Å | 7.3322(3) | 7.444(2) | 7.977(1) |
| *b*, Å | 10.014(1) | 8.518(2) | 8.656(1) |
| *c*, Å | 11.541(1) | 11.231(2) | 11.807(1) |
| α, deg | 113.22(1) | 97.45(2) | 69.06(1) |
| *β*, deg | 91.37(1) | 98.99(2) | 86.07(1) |
| *γ*, deg | 94.51(1) | 97.95(2) | 67.36(1) |
| *V*, Å$^3$ | 774.9(1) | 688.3(3) | 700.5(2) |
| *Z* | 2 | 1 | 1 |
| *λ*(Mo Kα), Å | 0.710 69 | 0.710 69 | 0.710 69 |
| *μ*(Mo Kα), cm$^{-1}$ | 14.71 | 18.08 | 16.02 |
| *ρ*(calcd), g cm$^{-3}$ | 1.76 | 1.78 | 1.74 |
| *T*, °C | 22 | 22 | 22 |
| $R^a$ | 0.039 | 0.054 | 0.059 |
| $Rw^b$ | 0.041 | 0.059 | 0.063 |

[a] $R = \sum|\Delta F|/\sum|F_o|$. [b] $Rw = [\sum w(\Delta F^2)/\sum wF_o^2]^{1/2}$.

was added and the pH adjusted to 1.8 with 0.1 M HCl. A polycrystalline powder appeared in a few minutes, which was washed, filtered and dried to constant weight at 70 °C. As a result, a violet powder of **1** was obtained. Blue crystals of compound **2** were obtained by slow evaporation of mother liquours at room temperature.

**Compound 4.** (a) Aqueous solutions of $CuCl_2\cdot 2H_2O$ (0.05 mmol, 5 mL) and HBIP (0.05 mmol, 5 mL) were added with stirring to an aqueous suspension of compound **1** (0.05 mmol, 25 mL), and the pH was adjusted to 6.5 with a solution of 0.1 M KOH. In a few minutes a green polycrystalline powder of **4** was obtained, which was filtered, washed with water and ethanol, and dried to constant weight at 70 °C. (b) To an aqueous suspension of compound **3** (0.05 mmol, 40 mL) was added 0.1 M KOH until pH 6.8; compound **4** was obtained as a polycrystalline powder from the resulting solution.

**X-ray Crystallographic Studies of 2, 3, and 5.** The selected prismatic crystals of the complexes were mounted on an Enraf-Nonius CAD4 single-crystal diffractometer and intensity measurements were carried out at room temperature using graphite-monochromated Mo Kα radiation ($\lambda$ = 0.710 69 Å). The unit cell dimensions were determined from the angular settings of 25 reflections. The intensity data were measured between the limits $1 < \theta < 25°$ using the $\omega/2\theta$ scan technique. Data were corrected for Lorentz and polarization effects. Empirical absorption corrections, following the procedure DIFABS[31] were applied.

The structures were solved by direct methods using the program SIR92.[32] In all cases, all non-hydrogen atoms were anisotropically refined by least-squares on F with the X-RAY76 System.[33] The hydrogen atoms were located by difference synthesis and kept fixed in the refinement with a common isotropic temperature factor. In the final stages an empirical weighting scheme was chosen as to give no trends in $\langle w\Delta^2F\rangle$ vs $\langle F_o\rangle$ and vs $\langle \sin\theta/\lambda\rangle$ using the program PESOS.[34] Atomic scattering factors and anomalous dispersion corrections were taken from reference.[35] Geometrical calculations were made with PARST.[36] The computer used was a VAX6410. Graphical representations were produced with ORTEP.[37]

**Complex 2.** Blue crystal with approximate size of 0.20 × 0.25 × 0.30 mm$^3$. The unit cell dimensions were determined in the range $8 < \theta < 14°$. 3041 reflections measured in the *hkl* ranges 0 to 8, −11 to 11, and −13 to 13. From the 2721 independent reflections 2368 were considered observed with $I > 2\sigma(I)$. Minimum and maximum correction coefficients of 0.768 and 1.299, with 226 refined parameters. After the final refinement: gof = 1.26, $\Delta\rho_{max}$ = 0.34 e Å$^{-3}$.

**Complex 3.** Green crystal with approximate size of 0.15 × 0.20 × 0.25 mm$^3$. The unit cell dimensions were determined in the range $9 < \theta < 16°$. 2726 reflections were measured in the *hkl* ranges 0 to 8, −10 to 10, and −13 to 13. From the 2420 independent reflections 1922 were considered observed with $I > 2\sigma(I)$. Minimum and maximum correction coefficients of 0.770 and 1.310, with 190 refined parameters. After the final refinement: gof = 1.05, $\Delta\rho_{max}$ = 0.51 e Å$^{-3}$.

**Complex 5.** Green crystal with approximate size of 0.20 × 0.20 × 0.30 mm$^3$. The unit cell dimensions were determined in the range $7 < \theta < 14°$. 2719 reflections were measured in the *hkl* ranges 0 to 9, −10 to 10, and −14 to 14. From the 2450 independent reflections 2295 were considered observed with $I > 3\sigma(I)$. Minimum and maximum correction coefficients of 0.769 and 1.227, with 199 refined parameters. After the final refinement: gof = 1.41, $\Delta\rho_{max}$ = 0.50 e Å$^{-3}$.

Other relevant parameters of the crystal structures are listed in Table 1. Selected bond distances and angles are listed in Table 2.

**Physical Measurements.** The IR spectra (KBr pellets) were recorded on a Pye Unicam SP 2000 spectrophotometer in the 4000−200 cm$^{-1}$ region. The diffuse reflectance spectra were obtained using a Perkin-Elmer Lambda 9 UV/vis/IR spectrophotometer. X-band polycrystalline powder EPR spectra were recorded on a Bruker ER 200D spectrometer equipped with a variable temperature device. Magnetic susceptibility was measured by means of a commercial SQUID magnetometer, Quantum Design model MPMS7 down to 1.8 K.

## Results

The versatility of HBIP as ligand and the selection of experimental conditions such as the different pH of crystallization and the appropriate molar ratios $HBIP/H_2C_2O_4/Cu(II)$ allowed the formation of five different compounds (**1**−**5**). Preparation of these compounds can be carried out by different strategies of synthesis either by direct mixing of the reagents or by interconversion among the obtained compounds. All synthetic sequences are shown in Scheme 1.

The water content of the complexes **1** and **4** has been verified by TGA, which indicates that all the water molecules are lost in one-step process at relatively low temperatures (60−120 °C). This indicates that the water molecules are not coordinatively bonded to the metal ions. The observed weight loss corresponds to the release of one water molecule for compound **1** and two for compound **4**. The X-ray powder pattern for compounds **1** and **4** differ significantly from those obtained for compounds **2**

(31) Walker, N.; Stuart, D. *Acta Crystallogr. Sect. A* **1983**, *39*, 158.
(32) Altomare A.; Burla, M. C.; Camalli, M.; Cascarano, G.; Giacovazzo, G.; Guagliardi, A.; Polidori, G. *J. Appl. Crystallogr.* **1994**, *27*, 435.
(33) Stewart, J. M.; Machin, P. A.; Dickinson, C. W.; Ammon, H. L.; Heck, H.; Flack, H. *The X-RAY76 System*; Technical Report TR-446; Computer Science Center, University of Maryland: College Park, MD, 1976.
(34) Martínez-Ripoll, M.; Cano, F. H. *PESOS Computer Program*; Instituto Rocasolano: CSIC, Madrid, Spain, 1975.
(35) *International Tables for X-ray Crystallography*; Kynoch Press: Birmingham, U.K., 1974; Vol. IV, pp 71 and 149.
(36) Nardelli, M. *Comput. Chem.* **1983**, *7*, 95.
(37) Johnson, C. K. *ORTEP*; Report ORN-3794; Oak Ridge National Laboratory: Oak Ridge, TN, 1965.

**Table 2.** Selected Bond Lengths (Å) and Angles (deg) for Complexes **2**, **3**, and **5**[a]

| | | | |
|---|---|---|---|
| Copper(II) Coordination Sphere | | | |
| Complex **2** | | | |
| Cu−O(3) | 1.971(3) | Cu−N(3) | 1.971(3) |
| Cu−O(4) | 1.989(2) | Cu−O(7) | 2.313(2) |
| Cu−N(2) | 1.961(2) | | |
| O(3)−Cu−O(4) | 83.3(1) | O(4)−Cu−N(3) | 95.7(1) |
| O(3)−Cu−N(2) | 90.6(1) | O(4)−Cu−O(7) | 89.7(1) |
| O(3)−Cu−N(3) | 178.9(1) | N(2)−Cu−N(3) | 90.1(1) |
| O(3)−Cu−O(7) | 86.0(1) | N(2)−Cu−O(7) | 104.1(1) |
| O(4)−Cu−N(2) | 164.6(1) | N(3)−Cu−O(7) | 94.7(1) |
| Complex **3** | | | |
| Cu−Cl | 2.505(2) | Cu−N(3) | 1.959(4) |
| Cu−O(3) | 2.016(4) | Cu−O(4)$^{i}$ | 2.041(3) |
| Cu−N(2) | 1.961(4) | | |
| Cl−Cu−O(3) | 93.8(1) | O(3)−Cu−N(3) | 167.1(2) |
| Cl−Cu−N(2) | 103.7(1) | O(3)−Cu−O(4)$^{i}$ | 81.9(1) |
| Cl−Cu−N(3) | 97.7(1) | N(2)−Cu−N(3) | 91.6(2) |
| Cl−Cu−O(4)$^{i}$ | 97.7(1) | N(2)−Cu−O(4)$^{i}$ | 157.9(2) |
| O(3)−Cu−N(2) | 91.3(2) | N(3)−Cu−O(4)$^{i}$ | 90.8(2) |
| Complex **5** | | | |
| Cu−O(3) | 2.001(3) | Cu−O(1)$^{ii}$ | 1.993(4) |
| Cu−N(2) | 1.971(3) | Cu−O(4)$^{i}$ | 2.266(3) |
| Cu−N(3) | 1.971(5) | | |
| O(3)−Cu−N(2) | 172.4(1) | N(2)−Cu−O(1)$^{ii}$ | 93.1(1) |
| O(3)−Cu−N(3) | 90.1(1) | N(2)−Cu−O(4)$^{i}$ | 94.3(1) |
| O(3)−Cu−O(1)$^{ii}$ | 89.5(1) | N(3)−Cu−O(1)$^{ii}$ | 160.7(1) |
| O(3)−Cu−O(4)$^{i}$ | 78.3(1) | N(3)−Cu−O(4)$^{i}$ | 103.1(1) |
| N(2)−Cu−N(3) | 89.7(2) | O(1)$^{ii}$−Cu−O(4)$^{i}$ | 95.7(1) |
| Oxalate Ligand | | | |
| Complex **2** | | | |
| O(3)−C(11) | 1.268(4) | O(6)−C(10) | 1.227(4) |
| O(4)−C(10) | 1.267(4) | C(10)−C(11) | 1.542(5) |
| O(5)−C(11) | 1.231(5) | | |
| O(4)−C(10)−O(6) | 126.6(3) | O(3)−C(11)−O(5) | 125.5(3) |
| O(4)−C(10)−C(11) | 115.1(3) | O(3)−C(11)−C(10) | 115.4(3) |
| O(6)−C(10)−C(11) | 118.3(3) | O(5)−C(11)−C(10) | 119.1(3) |
| Complex **3** | | | |
| O(3)−C(10) | 1.250(6) | C(10)−C(10)$^{i}$ | 1.543(7) |
| O(4)−C(10) | 1.232(6) | | |
| O(3)−C(10)−O(4) | 126.6(5) | O(4)−C(10)−C(10)$^{i}$ | 117.4(4) |
| O(3)−C(10)−C(10)$^{i}$ | 116.0(4) | | |
| Complex **5** | | | |
| O(3)−C(10) | 1.266(5) | C(10)−C(10)$^{i}$ | 1.585(4) |
| O(4)−C(10) | 1.222(5) | | |
| O(3)−C(10)−O(4) | 126.5(4) | O(4)−C(10)−C(10)$^{i}$ | 118.1(3) |
| O(3)−C(10)−C(10)$^{i}$ | 115.4(3) | | |

[a] Symmetry codes: (i) $-x, -y, -z$; (ii) $x-1, y, z$.

and **5** respectively. These results are consistent with the formulation proposed.

**Crystal Structure of 2.** The asymmetric unit consists of one isolated neutral [Cu(HBIP)($C_2O_4$)($OH_2$)] molecule and two noncoordinated water molecules. The structure of the complex is shown in Figure 1, together with the atomic numbering scheme. Figure 2 is a view of the unit cell contents illustrating the molecular packing.

The Cu(II) ion is five-coordinated with HBIP and oxalato entities acting as bidentate ligands and the water molecule as the fifth ligand. The corresponding Cu−O(ox) and Cu−N(imidazole) distances are of the same magnitude, ranging from 1.989(2) to 1.961(2) Å. The oxygen atom of the coordinated water molecule is at a larger distance (2.313(2) Å). The environment around the metal atom can be described as distorted square pyramidal (SP). As usual, the Cu(II) ion is displaced 0.134 Å from the best least-squares plane through the equatorial atoms toward the apical water oxygen O(7); while N(2), N(3), O(3), and O(4) deviate 0.113, −0.119, −0.123, and 0.101 Å

**Scheme 1**[a]

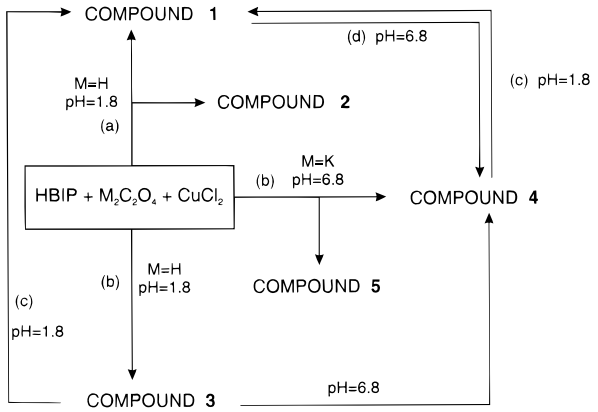


[a] Legend: (a) 1:1:1 ratio; (b) 1:0.5:1 ratio; (c) addition of 0.5 equiv of $H_2C_2O_4$; (d) addition of 1 equiv of $CuCl_2$ and 1 equiv of HBIP.

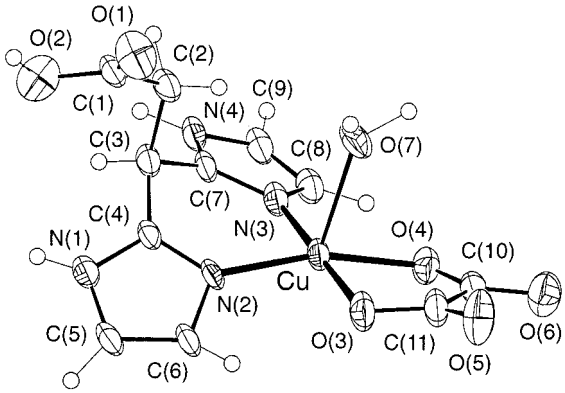


**Figure 1.** ORTEP drawing of the monomeric entity of compound **2** showing the atom-labeling scheme. Thermal ellipsoids are drawn at the 50% probability level.

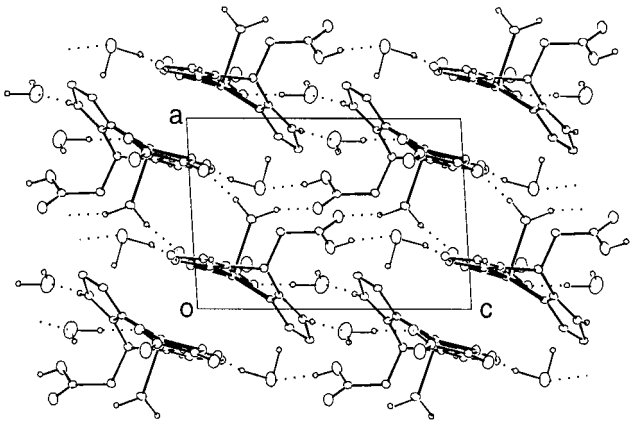


**Figure 2.** Crystal packing of compound **2** as projected on the *ac* planes. Hydrogens of carbon atoms have been omitted.

respectively, from this plane, showing a significant tetrahedral distortion. This distortion of the metal environment is also evident from the values of the angles around Cu(II) in the basal plane (ranging from 83.3(1) to 95.7(1)°). The distortion of the coordination polyhedron around the copper atom can be quantified by using the approach of Muetterties and Guggenberger.[38] In this method, the dihedral angles between adjacent faces (known as the shape-determining angles $e_1$, $e_2$, and $e_3$) are calculated in order to describe an intermediate geometry.

(38) Muetterties, E. L.; Guggenberger, L. J. *J. Am. Chem. Soc*. **1974**, *96*, 1748.

**Table 3.** Hydrogen Contacts in the Crystal Structures[a]

| Complex **2** | | Complex **3** | | Complex **5** | |
|---|---|---|---|---|---|
| X−H···Y | X···Y, Å | X−H···Y | X···Y, Å | X−H···Y | X···Y, Å |
| O(2)···O(8) | 2.644(4) | O(2)···O(5) | 2.619(6) | O(6)···O(7) | 2.75(1) |
| O(9)···O(3) | 2.977(5) | N(1)···O(1)$^{i}$ | 2.823(6) | N(4)···O(5) | 2.93(1) |
| N(1)···O(9)$^{i}$ | 2.752(4) | N(4)···Cl$^{ii}$ | 3.148(5) | N(1)···O(5)$^{i}$ | 2.89(1) |
| N(4)···O(5)$^{ii}$ | 2.867(3) | O(5)···O(4)$^{iii}$ | 3.049(5) | O(5)···O(7)$^{ii}$ | 2.73(1) |
| O(7)···O(1)$^{iii}$ | 2.812(4) | O(5)···Cl$^{iv}$ | 3.055(5) | O(7)···O(7)$^{ii}$ | 2.60(1) |
| O(7)···O(6)$^{iv}$ | 2.788(4) | | | O(5)···O(4)$^{iii}$ | 2.94(1) |
| O(8)···O(4)$^{v}$ | 2.903(4) | | | O(6)···O(1)$^{iv}$ | 2.87(1) |
| | | | | O(7)···O(3)$^{v}$ | 2.75(1) |

[a] Symmetry codes for each complex are as follows: for **2**, (i) $-x, -y+1, -z+1$; (ii) $x, y+1, z$; (iii) $-x+1, -y+1, -z+1$; (iv) $-x+1, -y, -z$; (v) $x, y+1, z+1$; for **3**, (i) $-x+2, -y, -z+1$; (ii) $x+1, y, z$; (iii) $-x+1, -y, -z+1$; (iv) $-x+1, -y-1, -z+1$; for **5**, (i) $-x+1, -y, -z+1$; (ii) $-x+1, -y+1, -z$; (iii) $-x, -y+1, -z$; (iv) $-x+1, -y, -z$; (v) $x+1, y, z$.

The key shape-determining angle, $e_3$, is 0.0° for an ideal square pyramid (SP) and 53.1° for an ideal trigonal bipyramid (TBP). For the considered compound, $e_3 = 13.5°$, indicating a strong predominance of the SP form.

The Cu−N distances compare well with the bond lengths in other Cu(II)−imidazole complexes.[22,27,39−42] On the other hand, the Cu−O(oxalato) distances are very close to those reported for other copper complexes involving terminal oxalato.[43,44]

All the relevant parameters for the HBIP ligand are in good agreement with the data obtained for related structures.[27,45,46] As usually observed, each imidazole ring is planar (the largest deviation from the best plane being 0.003 Å). The imidazole moieties of each ligand however are not coplanar, with a dihedral angle of 40.9(1)°. This value differs significantly from that found in the free ligand[45,46] and can be related to the coordination to the metal. The angle between the carboxylate group O(1)−O(2)−C(1)−C(2), which is planar (largest deviation 0.003 Å), and the imidazole rings is 41.3(1)° for the [N(3)−C(7)−N(4)−C(9)−C(8)] ring and 71.7(1)° for the [N(2)−C(4)−N(1)−C(5)−C(6)] one.

The oxalato group is not planar, with deviations up to 0.154 Å from the least-squares plane. This distortion is associated with a twisting about the C(10)−C(11) bond which leads to a dihedral angle of 10.9(2)° between the O(3)−C(11)−O(5) and O(4)−C(10)−O(6) groups. A similar distortion is also observed in the other terminal oxalato ligands.[47] The C−O bond distances satisfy the trend $C-O_{coord} > C-O_{uncoord}$, as expected from the polarization of the charge density toward the metal-bonded oxygen atoms. Furthermore, the C−O bond lengths are also affected by H-bonding.

Hydrogen bonding (involving N−H groups and oxygen atoms of the HBIP, oxygen atoms of the oxalato, and water molecules) appears to be important for the stabilization of the crystal lattice. The characteristics of the hydrogen bond network are given in Table 3.

Of this set of hydrogen bonds we should highlight those involving the hydrogen atoms of the coordinated water molecule with the O(1) from the carboxylic group and O(6) from the oxalato group. The hydrogen bond O(7)−H···O(1) gives dinuclear units between two complex molecules related by the inversion center at ($^1/_2$, $^1/_2$, $^1/_2$) with a Cu−Cu distance of 8.94(7) Å, whereas the hydrogen bond O(7)−H···O(6) gives dinuclear units joining also two complex molecules, related by the inversion center at ($^1/_2$, 0, 0), with a Cu−Cu distance of 7.33(5) Å. Taking into account both interactions, the complex molecules form infinite chains in zigzag parallel to the *z* axis (Figure 2).

**Crystal Structure of 3.** The structure of this complex is made up of centrosymmetric binuclear [{Cu(HBIP)Cl}$_2$($\mu$-$C_2O_4$)] units and noncoordinated water molecules. A drawing of the dimeric structure showing the labeling scheme is given in Figure 3. The two copper atoms are linked through a bis-bidentate oxalato group leading to a metal−metal separation of 5.28(3) Å. The coordination stereochemistry of the $CuN_2O_2Cl$ chromophore is approximately SP. The basal coordination positions are occupied by two oxalato oxygen atoms, O(3) and O(4)$^{i}$, and two nitrogen atoms of the bidentate HBIP ligand, N(2) and N(3). The Cu−N and Cu−O bond distances range from 1.959(4) to 2.041(3) Å. The apical position is occupied by the chlorine atom at a larger distance (2.505(2) Å). The four basal atoms are coplanar showing a slight but significant tetrahedral distortion. In fact, the O(3) and N(3) atoms are displaced by 0.078(4) and 0.092(4) Å on one side of the $CuN_2O_2$ least-squares plane while the O(4)$^{i}$ and N(2) atoms are 0.077(4) Å and 0.093(4) Å on the other side ($i = -x, -y, -z$). The copper atom is 0.298(1) Å out of that plane toward the apex. The Cu−Cl distance is normal and is in the range observed for the copper(II) compounds having Cl at the axial site.[48]

The distortion from SP geometry can be related to the O(3)−Cu−O(4)$^{i}$ (81.9(1)°), N(2)−Cu−N(3) (91.6(2)°), O(3)−Cu−N(2) (91.3(2)°), and N(3)−Cu−O(4)$^{i}$ (90.8(2)°) angles, which are close to those expected for a SP geometry (90°). The value of $e_3 = 9.88°$ is consistent with a predominance of the SP geometry over the TBP one.

The Cu−O(oxalato) distances and the O−Cu−O angles in the five-membered rings of the bis-bidentate oxalato are very close to those reported for other oxalato bridged Cu(II) binuclear complexes,[2,49−52] but they are slightly different to those involv-

(39) Soto, L.; Legros J. P.; Sancho, A. *Polyhedron* **1988**, *7*, 307.
(40) Orpen, A. G.;. Brammer, L.; Allen, F. H.; Kennard, O.; Watson, D. G.; Taylor, R. *J. Chem. Soc., Dalton Trans.* **1989** (Suppl. 1).
(41) Oberhausen, K. J.; Richardson, J. F.; Buchanan, R. M.; McCusker, J. K.; Hendrickson, D. N.; Latour, J. M. *Inorg. Chem*. **1991**, *30*, 1357.
(42) Antolini, L.; Battaglia, L. P.; Bonamartini Corradi, A.; Marcotrigiano, G.; Menabue, L.; Pellacani, G. C.; Saladini, M. *Inorg. Chem*. **1982**, *21*, 1391.
(43) Fitzgerald, W.; Foley, J.; McSweeney, D.; Ray, N.; Sheahan, D.; Tyagi, S.; Hathaway, B.; O'Brien. P. *J. Chem. Soc., Dalton Trans*. **1982**, 1117.
(44) Suarez-Varela, J.; Soto, L.; Legros, J. P.; Esteve, C.; Garcia, J. *Polyhedron* **1988**, *7*, 229.
(45) Gimeno, B.; Soto, L.; Sancho, A.; Dahan, F.; Legros, J. P. *Acta Crystallogr*. **1992**, *C48*, 1671.
(46) Gimeno, B.; Sancho, A.; Soto, L.; Legros, J. P. *Acta Crystallogr*. **1996**, *C52*, 1226.
(47) Román P.; Guzmán-Miralles, C.; Luque, A., Beitia, I.; Cano, J.; Lloret, F.; Julve, M.; Alvarez, S. *Inorg. Chem*. **1996**, *35*, 3741.
(48) Rao, S. P. S.; Varughese, K. Y.; Manohar, H. *Inorg. Chem*. **1986**, *25*, 734.
(49) Soto, L.; Garcia, J.; Escriva, E.; Beneto, M.; Dahan, F.; Tuchagues, J. P.; Legros, J. P. *J. Chem. Soc., Dalton Trans*. **1991**, 2619.

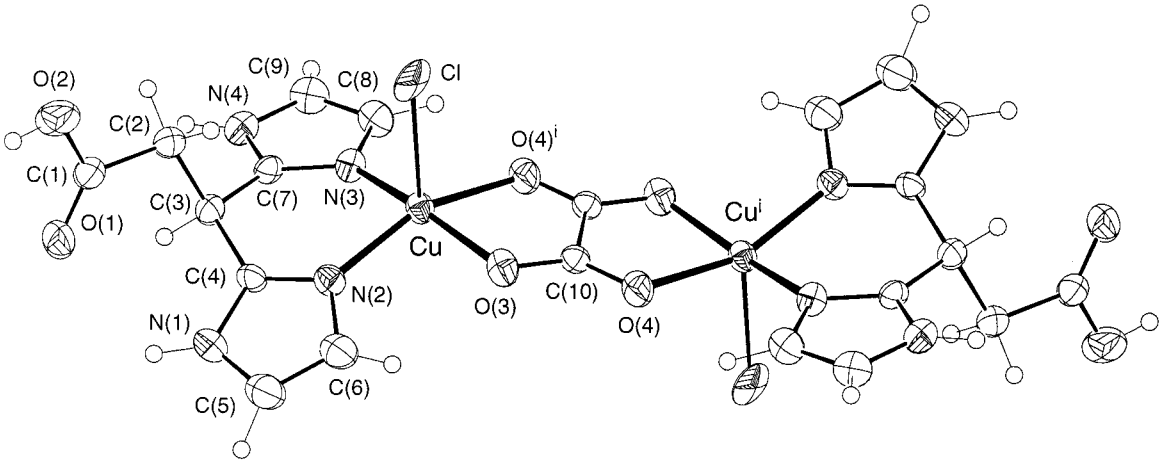


**Figure 3.** ORTEP drawing of the dimeric entity of compound **3** showing the atom-labeling scheme. Thermal ellipsoids are drawn at the 50% probability level. i = $-x, -y, -z$.

ing the terminal oxalato (complex **2**).[43,44] The oxalato anion is planar due to the inversion center halfway along the bond C(10)−C(10)$^{i}$. The Cu−N(imidazole) distances are very close to those observed in parent compounds. Interatomic distances and bond angles in the HBIP are in good agreement with previously reported data. The imidazole rings are planar as expected with deviations from the mean planes not greater than 0.005(6) Å. However, they are not coplanar, with a dihedral angle of 25.8(2)° between the imidazole rings.

As usually observed, the carboxylate group is planar (largest deviation 0.016 Å), the angles between this group and the imidazole rings are 89.4(2) and 75.7(2)° with [N(3)−C(7)−N(4)−C(9)−C(8)] and [N(2)−C(4)−N(1)−C(5)−C(6)] rings, respectively.

The binuclear entity is folded as indicated in Figure 3. The basal coordination plane makes an angle $\gamma = 11.5(1)°$ with the mean plane of the oxalato ligand. As a result, the binuclear complex displays a stair-like structure. Notwithstanding, because of the out-of-plane position of the copper atoms, the central [Cu($C_2O_4$)Cu] core is nearly planar, with the copper atoms deviating only 0.0045 Å from the oxalato plane.

The characteristics of the hydrogen bonds are given in Table 3. All the oxygen atoms (excluded the O(3) atom from the oxalato group), N−H groups and Cl atoms are involved in the hydrogen-bond network.

The hydrogen bond set leads to the three-dimensional network shown in Figure 4. However, it should be stressed that the structure can be viewed as planes of dimeric molecules perpendicular to the *b* axis on the *ac* faces, which are linked by the H bonds of the water molecules. The H bonds defining these planes are those of N−H groups from both imidazoles with a shortest Cu−Cu distance of 7.444(3) Å between two dimers related by the N(4)−H bond. The water molecules join the planes acting as H-acceptor of a strong H-bond with O(2) atom in the carboxylic group and as H-donor with O(4) and Cl atoms from differents neighboring molecules.

**Crystal Structure of 5.** The structure of complex can be viewed as made up of [(BIP)Cu($C_2O_4$)Cu(BIP)] units (Figure 5) and noncoordinated water molecules. The compound exhibits a structure built of ladder-like chains running along the *a* direction, which are connected through H-bonds involving the water molecules. In these chains the rungs are constituted by the neutral dinuclear centrosymmetric [(BIP)Cu($C_2O_4$)Cu(BIP)] units where the oxalato group bridges two copper atoms in a bis-bidentate fashion and the BIP acts as a tridentate ligand, connecting through their carboxylate groups these dimeric units along the *a* axis.

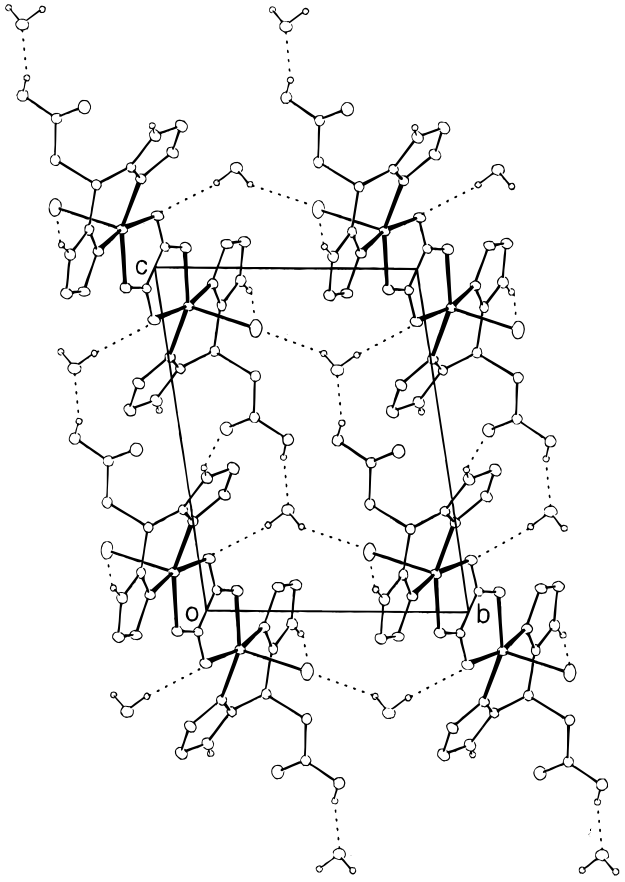


**Figure 4.** Crystal packing of compound **3** as projected on the *bc* planes. Hydrogens of carbon atoms have been omitted.

The copper atom is involved in a five-coordinated $CuN_2O_2O'$ chromophore. The coordination geometry is intermediate between SP and TBP. If the complex is considered as SP, then one oxalato oxygen O(4)$^{i}$ occupies the apical position with the other oxalato oxygen atom O(3), nitrogen atoms and O(1)$^{ii}$ from the carboxylate group in the basal plane. The Cu−N and Cu−O

(50) Julve, M.; Verdaguer, M.; Gleizes, A.; Philoche-Levisalles, M.; Kahn, O. *Inorg. Chem.* **1984**, *23*, 3808.
(51) Decurtins, S.; Schmalle, H. W.; Schneuwly, P.; Zheng, L. M.; Ensling, J.; Hauser, A. *Inorg. Chem.* **1995**, *34*, 5501.
(52) Felthouse, T. R.; Laskowski, E. J.; Hendrickson, D. N. *Inorg. Chem.* **1977**, *16*, 1077.

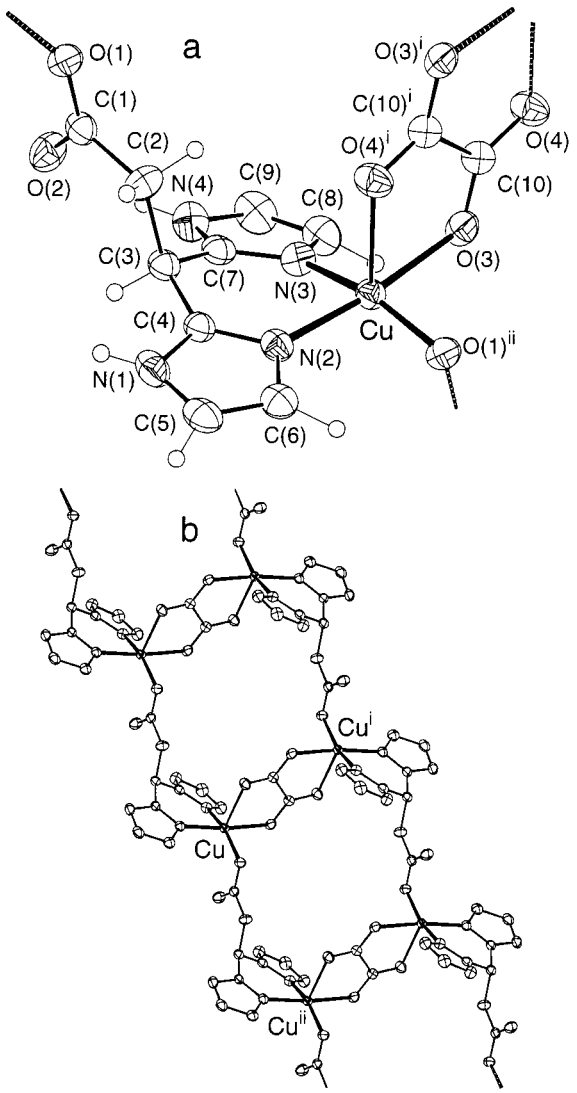


**Figure 5.** ORTEP drawings of compound **5** showing: (a) the atom-labeling scheme and (b) the polymeric chains in the crystal structure. Thermal ellipsoids are drawn at the 50% probability level. i = $-x$, $-y$, $-z$; ii = $x - 1$, $y$, $z$.

distances in the basal plane range from 1.971(5) to 2.001(3) Å and are significantly shorter than the apical bond length (Cu−O(4)$^{i}$ = 2.266(3) Å). Deviations from a best least-squares plane through N(2)−N(3)−O(3)−O(1)$^{ii}$ are 0.239(4), −0.273(3), 0.181(4), and −0.227(4) Å, respectively. The copper atom deviates by 0.082(1) Å toward the axial ligand. The angles around copper in the basal plane vary from 78.3(1) to 93.1°(1). These values show that the distortion from idealized SP geometry is appreciable. Viewing the complex as distorted TBP, N(3), O(1)$^{ii}$, and O(4)$^{i}$ define the equatorial plane and N(2) and O(3) in axial positions. Cu (II) is 0.064(1) Å out of this equatorial plane in the direction of N(2) and the trigonal axis does not show too much distortion from linearity, O(3)−Cu−N(2) angle being 172.4(1)°. However, the angles in the equatorial plane depart significantly from the theoretical 120° value, with values of 95.7(1), 103.1(1), and 160.7(1)°. Certainly, the value of the $e_3$ angle (26.2°) indicates a strong distortion of the polyhedron.

The oxalato bridge is asymmetrically coordinated with one short Cu−O(3) bond (2.001(3) Å) and one long Cu−O(4)$^{i}$ bond (2.266(3) Å). The C−C bond of 1.585(4) Å is significantly longer than the values of 1.50−1.54 Å usually observed in the

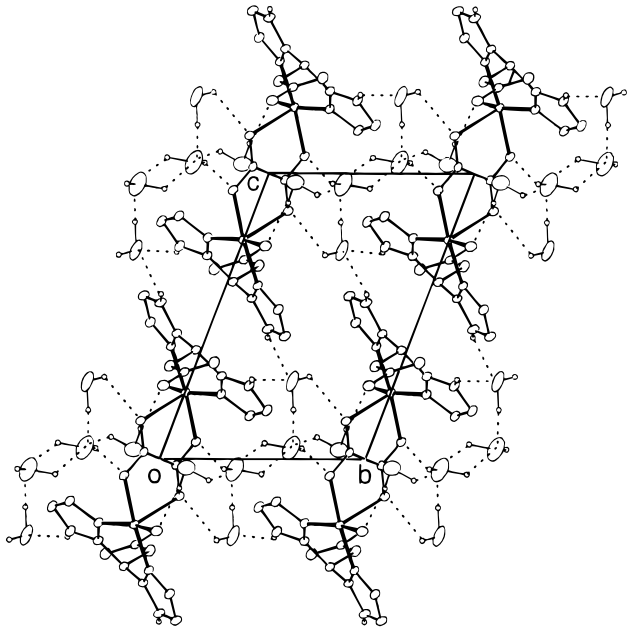


**Figure 6.** Crystal packing of compound **5** as projected on the *bc* planes. Hydrogens of carbon atoms have been omitted.

coordinated oxalato. The O(4)$^{i}$−Cu−O(3) angle in **5** is 78.3(1)°, significantly lower than in **2** (83.3(1)°) and **3** (81.9(1)°).

The two Cu−N bonds are identical and compare well with the bond lengths in **2** and **3**. The bond distances and angles within the BIP ligand have normal values. The dihedral angle between the two planar imidazole rings is 21.7(1)°. This value differs significantly from that found in the free ligand as well as in compound **2**. The carboxylic group is planar (largest deviation 0.010(4) Å), the dihedral angles between this group and imidazole rings being 70.1(1)° and 86.7(1)° for [N(3)−C(7)−N(4)−C(9)−C(8)] and [N(2)−C(4)−N(1)−C(5)−C(6)], respectively.

As in the compound **3** the centrosymmetric oxalato bridge is planar and forms an angle of 91.1(1)° with respect to the equatorial plane of the copper polyhedron.

The Cu−Cu separation through the oxalato bridge inside the binuclear fragment is 5.52(1) Å, while the copper−copper separation between Cu(II) ions belonging to two different molecules along the chains is 7.977(1) Å.

The hydrogen contacts listed in Table 3 mainly determine the crystal packing showed in Figure 6. The polymeric chains running along *a* direction are connected by a three-dimensional network of hydrogen bonds involving water molecules, nitrogen atoms, and O(1) from BIP ligands and oxalato oxygen atoms.

**IR and Electronic Spectra.** The IR spectra of all complexes show strong and broad bands in the 3610−3280 cm$^{-1}$ range assignable to $\nu$(OH) stretching vibrations of lattice and/or coordinated water molecules.[54] The observed position of the $\nu$(OH) bands is in agreement with the participation of water molecules in strong hydrogen bonds. Differences in this region between complexes **1** versus **2** and **4** versus **5** are consistent with the different water content and this is further substantiated by the results of elemental and thermal analyses. It is of interest to note that complex **1** lacks the band at 3480 cm$^{-1}$ assigned in **2** to coordinated water. The N−H stretching vibrations of complexes **1**−**5** appear in the 3155−3020 cm$^{-1}$ region and their

(53) Soto, L.; Garcia, J.; Escriva, E.; Legros, J.-P.; Tuchagues, J.-P.; Dahan, F.; Fuertes, A. *Inorg. Chem.* **1989**, *28*, 3378.
(54) Nakamoto, K. *Infrared and Raman Spectra of Inorganic and Coordination Compounds*, 4th ed.; Wiley: New York, 1986.

frequencies are consistent with the existence of hydrogen bond between imidazole N−H and other groups.[27] In the 1600−800 $cm^{-1}$ region the spectra display a large number of absorptions which correspond to the coexistence of the imidazole, oxalato, and carboxylate moieties, preventing a definitive assignment in some cases. Nevertheless, a comparison between the spectra parameters (number, position, broadness and intensity of bands) reveals that they can be used to differentiate among the coordination modes of carboxylate and oxalato groups. Complexes **1**, **2**, and **3** exhibit one $\nu_{as}$(COO) band at ca. 1700 $cm^{-1}$ [$\nu$(COOH) un-ionized];[55] while, this band is missing in the spectra of **4** and **5**, indicating the loss of the COOH proton. It must be stressed that the broadness of this band for the compounds **1** and **2** is the result of overlapping between $\nu_{as}$(COO) of un-ionized carboxylate group and the same vibration of the oxalato group acting in a bidentate fashion.[56−58] For complexes **1** and **2** the other relevant absorptions are medium-intensity bands at 1415 and 1280 $cm^{-1}$ [($\nu_s$(COO)] consistent with a bidentate oxalato. For complexes **3**, **4** and **5** these bands are shifted indicating that the oxalato group acts in a different manner. It is interesting that complexes **4** and **5** exhibit a single and very strong peak at 1400 $cm^{-1}$ assignable to $\nu_s$(COO) that is lacking in the rest of the complexes, this frequency being consistent with a monodentate coordination of the carboxylate group in both complexes.[54,59,60] These spectral features are in agreement with the crystal structure analyses for complexes **2**, **3**, and **5** described above. Owed to the lack of crystallographic data for compounds **1** and **4**, the above assignments can be used as diagnostic of different coordination modes of oxalato and carboxylate groups in these complexes, since the IR spectra of **1** versus **2** and **4** versus **5** are nearly superimposable, the only differences being the bands assigned to the v(OH) of water. On the basis of the above considerations, it can be concluded that (a) in complex **1** the carboxylate group is protonated (band at 1700 $cm^{-1}$) and the oxalato group acts in a bidentate fashion (bands at 1415 and 1280 $cm^{-1}$); (b) in compound **4**, the carboxylate group is coordinated to copper ion (band at 1700 $cm^{-1}$ is lacking and a band appear at 1400 $cm^{-1}$) and the oxalato acts as a bis-bidentate ligand[47,57,61−63] as evidenced by the crystallographic study for complex **5** described above. No peak can be assigned unambiguously to metal−ligand vibrations in the region below 600 $cm^{-1}$, since the ligands themselves have several absorptions in this region.

The diffuse reflectance spectra of compounds **2**, **3**, **4**, and **5** exhibit a very broad absorption in the visible region with a maximum centered between the 13 800 and 15 300 $cm^{-1}$ range, which is consistent with a five-coordinated copper(II) chromophore with an intermediate geometry between ideal square pyramid and trigonal bypiramid.[64,65] For complex **1** the position of the maximum at 16 400 $cm^{-1}$ is consistent with the tetracoordination of a nearly square planar geometry. This fact is in accordance with the thermal analysis and EPR spectrum.

Besides the d−d bands, the spectra display a more intense bands centered at ca. 31 000 and 37 000 $cm^{-1}$, which can be assigned to $\pi$(imidazole) → Cu(II) ($d_{x^2-y^2}$, $d_{z^2}$) LMCT and internal ligand $\pi \rightarrow \pi^*$ transitions, respectively.

**Electron Paramagnetic Resonance Spectra.** The X-band room-temperature EPR spectrum of polycrystalline samples of compound **2** is axial giving $g_{||} = 2.25$ and $g_{\perp} = 2.07$ ($g_{av} = 2.13$) and hyperfine structure is not observed. These g-values are consistent with the distorted SP $CuN_2O_2O'$ chromophores present in the compound and indicate a basically $d_{x^2-y^2}$ ground state for the Cu(II) ion. On the other hand, the spectrum of compound **1** is also axial but with lower $g$ values, leading to $g_{||} = 2.21$ and $g_{\perp} = 2.06$ ($g_{av} = 2.11$), thus confirming the presence of $CuN_2O_2$ chromophores of geometry close to square planar, as suggested by electronic spectroscopy and TGA analysis.

Compound **3** exhibits a weak and very broad (350 G peak-to-peak) but asymmetric X-band EPR signal at room temperature. In addition, a very weak signal in the $\Delta M_s = \pm 2$ region is also observed, indicating low-dimensional magnetic interactions between copper(II) ions. The low intensity of the $\Delta M_s = \pm 1$ signal and the presence of the half-field feature agree well with the dimeric nature of the compound and the relatively high value of the antiferromagnetic coupling parameter. When lowering the temperature the spectrum narrows, and below 120 K some features corresponding at least to four resonances are clearly resolved in the $g = 2$ region, whereas the $g = 4$ signal is better observed. However, below 30 K the $g = 4$ signal disappears and the principal region evolves into a weak axial spectrum with $g_{||} = 2.28$ and $g_{\perp} = 2.07$. According to the magnetic behavior of the compound this low temperature spectrum must be associated with some amount of paramagnetic impurity present. Interestingly enough are the spectra between 40 and 80 K. In this range two peaks are clearly seen at lower and higher field from the $g_{\perp}$ signal of the monomer impurity, together with two weak shoulders in the $g_{||}$ region. These features can be associated with a triplet state with nonnegligible zero-field splitting, and can be generated with $g_z = 2.28$, $g_x = g_y = 2.07$, $|D| = 240$ G and $E$ practically zero ($D$ and $E$ are the zero-field splitting parameters).[66] In any case the $g$ values are consistent with $CuN_2O_2Cl$ chromophores of distorted SP geometry and indicate a basically $d_{x^2-y^2}$ ground state for the Cu(II) ions. Taking the crystallographic Cu−Cu distance of 5.28 Å, a dipolar contribution to $D$ of 203 G is expected,[67] thus suggesting that the zero-field splitting must be mainly of dipolar origin. The slight deviation from the experimental value could be due to an small exchange contribution, although these values must be taken carefully because the existence of noncollinear **g** and **D** tensors could lead to some errors in the interpretation of powder spectra.

Compound **4** exhibits also a weak and broad (400−450 G peak-to-peak) EPR signal at room temperature in the $g = 2.11$ region, without any structure. Upon lowering the temperature, the signal intensity diminishes and vanishes below 20 K, indicating relatively strong antiferromagnetic interactions between the copper(II) ions (see below). At lower temperatures only a weak axial signal remains corresponding to some amount of paramagnetic species.

Similarly to compound **2**, the X-band spectrum of **5** is axial

(55) Van Albada, G. A.; Haasnoot, J. G.; Reedijk, J.; Biagini-Cingi, M.; Manotti-Lanfredi, A. M.; Ugozzoli, F. *Polyhedron* **1995**, *14*, 2467.
(56) Fujita, J.; Martell, A. E.; Nakamoto, K. *J. Chem. Phys.* **1962**, *36*, 324.
(57) Gleizes, A.; Julve, M.; Verdaguer, M.; Real, J. A.; Faus J.; Solans. X. *J. Chem. Soc., Dalton Trans.* **1992**, 3209.
(58) Román P.; Luque, A.; Guzmán-Miralles, C.; Beitia, I. *Polyhedron* **1995**,*14*, 2863.
(59) Abuhijleh, A. L.; Woods, C. *Inorg. Chim. Acta* **1992**, *194*, 9.
(60) Battaglia, L. P.; Corradi, A. B.; Menabue, L.; Pellacani, G. C.; Prampolini, P.; Saladini, M. *J. Chem. Soc., Dalton Trans*. **1982**, 781.
(61) Battaglia, L. P.; Bianchi, A.; Corradi, A. B.; García-España, E.; Micheloni, M.; Julve, M. *Inorg. Chem.* **1988**, *27*, 4174.
(62) Curtis, N. F. *J. Chem. Soc*. **1963**, 4109.
(63) Curtis, N. F. *J. Chem. Soc. A* **1968**, 1584.
(64) Lever, A. B. P. *Inorganic Electronic Spectroscopy*, 2nd ed.; Elsevier: Amsterdam, 1986.
(65) Hataway, B. J. *Coord. Chem. Rev*. **1983**, *52*, 87.
(66) Wasserman, E.; Synder, L. C.; Yager, W. A. *J. Chem. Phys*. **1964**, *41*, 1763.
(67) Eaton, S. S.; More, K. M.; Sawant, B. M.; Eaton, G. R. *J. Am. Chem. Soc*. **1983**, *105*, 6560.

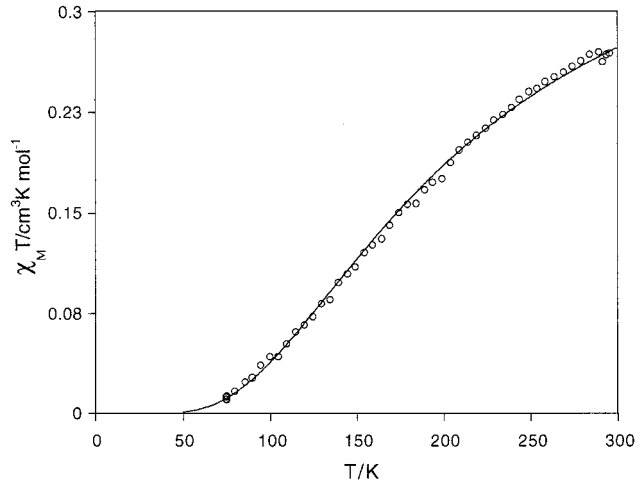


**Figure 7.** Plot of temperature-dependence of the $\chi_M T$ product for compound **3**.

giving $g_{||} = 2.29$ and $g_{\perp} = 2.07$ ($g_{av} = 2.14$), indicating a basically $d_{x^2-y^2}$ ground state for the Cu(II) ion present in the $CuN_2O_2O'$ chromophores of distorted SP geometry.

**Magnetic Properties.** The magnetic study of compounds **1** and **2** shows that in the studied temperature range (1.8−300 K) the $\chi_M T$ product is nearly constant and the whole susceptibility data can be nicely fitted to the Curie−Weiss expression $\chi_M = C/(T - \theta)$, affording $C = 0.415$ cm$^3$ mol$^{-1}$ ($g = 2.10$), $\theta = -0.17$ K for **1** and $C = 0.422$ cm$^3$ mol$^{-1}$ ($g = 2.12$), $\theta = -0.14$ K for **2**. The very small absolute value of the Weiss correction could suggest a very weak antiferromagnetic interaction between the copper(II) ions in both compounds. This interaction, if present, could only be detected unambiguously at very low temperatures.

The magnetic behavior of compound **3** is illustrated in Figure 7 by means of a plot of $\chi_M T$ vs the temperature in the range 77−300 K. Upon cooling from room temperature, the $\chi_M T$ product decreases continuously, thus indicating a strong antiferromagnetic interaction between copper atoms in the dimers. The experimental data were fitted to the Bleaney−Bowers equation modified according to Kahn and co-workers[68] to take into account some paramagnetic impurity ($\rho$). The least-squares fitting procedure led to $2J = -265$ cm$^{-1}$, $g = 2.13$, and $\rho = 0.01$, with an agreement factor of $R = 7.6 \times 10^{-4}$ ($R$ is defined as $\sum[(\chi_M)_{obsd} - (\chi_M)_{calcd}]^2/\sum[(\chi_M)_{obsd}]^2$). Since the diamagnetic correction is of the same order of magnitude as the uncorrected molar susceptibility, the uncertainty in the corrected values of $\chi_M$ is large, affording estimated $2J$ values reliable only within 5−10%.[69]

Figure 8 shows the magnetic behavior of compound **4**. Upon cooling, the magnetic susceptibility increases until a maximum, is reached at ca. 90 K, followed by a decrease of $\chi_M$, indicating medium-strong antiferromagnetic interactions between the copper(II) ions. From the position of the maximum, a value of ca. −100 cm$^{-1}$ could be estimated for the antiferromagnetic coupling constant ($2J$). The least-squares fitting of the experimental data to the Bleaney−Bowers equation (see discussion) affords $2J = -108$ cm$^{-1}$, $g = 2.15$, and $\rho = 0.02$, with an agreement factor of $R = 6.8 \times 10^{-4}$.

The magnetic behavior of the compound **5** is displayed in Figure 9. Plot of $\chi_M T$ vs the temperature exhibits a significant decrease at $T < 20$ K, corresponding to a variation of $\mu_{eff}$

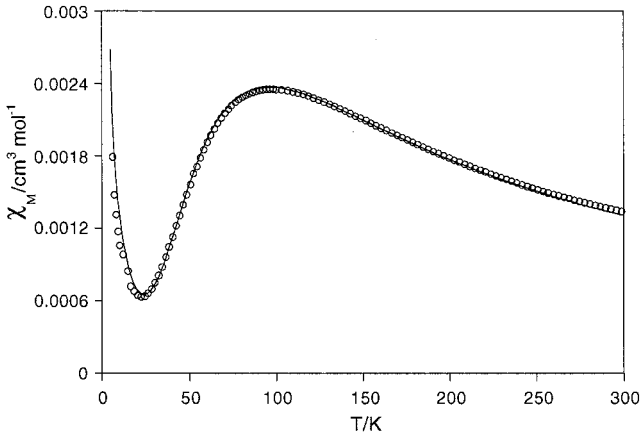


**Figure 8.** Plot of magnetic susceptibility vs temperature for compound **4**

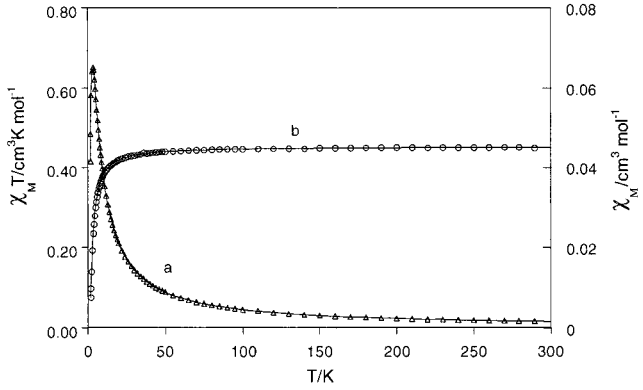


**Figure 9.** Thermal variation of magnetic susceptibility (a) and of $\chi_M T$ product (b) for compound **5**.

between 1.82 $\mu_B$ (at 20 K) and 1.15 $\mu_B$ (at 1.8 K) per copper atom. Otherwise, a maximum in the $\chi_M$ vs the temperature curve is observed ($T_{max}$ ca. 3.5 K). This behavior provides evidence of the presence of weak antiferromagnetic coupling between the copper(II) ions.

As has been discussed previously, the most outstanding structural features of compound **5** is the existence of ladder-like chains. Hence, in this compound the spin problem involves strictly two exchange-coupling constants, $J_1$ and $J_2$, for the interaction along the rungs (the *intradimeric* interaction) and along the chains (the *interdimeric* one), respectively. Nevertheless, taking into account the topology of the framework bridges, it may be assumed that the *intradimeric* interaction is the predominant exchange pathway and must be much stronger than that propagated through the propionate bridges (interdimeric), i.e., $|J_1| \gg |J_2|$. According to the limit function proposed by Coffman and Buettner[70] for long-range exchange interactions, which has the form $-2J = 1.35 \times 10^7 \exp(-1.8R)$, for an *interdimer* exchange pathway distance of ca. 11 Å the absolute $J_2$ value would be expected to be less than 0.05 cm$^{-1}$. In addition, this extended pathway involves two C−C $\sigma$ bonds, that offer a very poor support for the interactions.[1,71] Therefore, the effectiveness of the interdimeric pathway to support significant magnetic exchange interactions between the copper atoms may be considered as negligible, assuming $|J_2| \sim 0$. Thus, from a magnetic point of view, compound **5** might be considered as an assembly of "quasi" isolated dimers and, accordingly, its

(68) Journaux, Y.; Sletten, J.; Kahn, O. *Inorg. Chem.* **1985**, *25*, 4063.
(69) O'Connor, C. *Prog. Inorg. Chem.* **1982**, *20*, 203.
(70) Coffman, R. E.; Buettner, G. R. *J. Chem. Phys.* **1979**, *83*, 2387.
(71) Hay, P. J.; Thibeault, J. C.; Hoffmann, R. *J. Am. Chem. Soc.* **1975**, *97*, 4886.

**Chart 1**

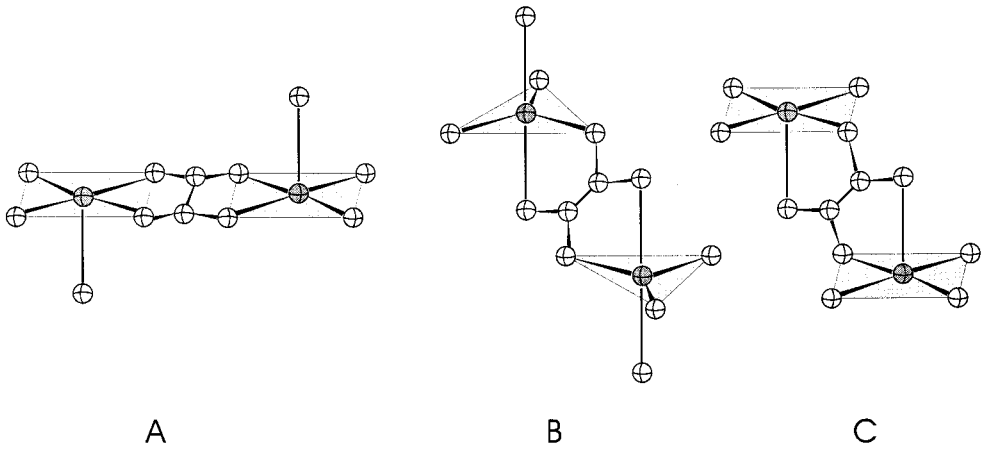


magnetic behavior could be described by means of a dimer exchange equation. With these considerations in mind, we have used the expression (eq 1) derived from the exchange Hamiltonian $\hat{H} = 2J(\hat{S}_1 \cdot \hat{S}_2) + g\mu_B H(\hat{S}_1 + \hat{S}_2)$ for a pair of exchange-coupled $S = {}^1/_2$ ions, that consider the external field.[72]

$$\chi_M = [Ng\mu_B \sinh(g\mu_B H/kT)]\{H[\exp(-2J/kT) + 2\cosh(g\mu_B H/kT) + 1]\}^{-1} + N\alpha \quad (1)$$

Residual *interdimeric* interactions through the propionate bridges were accounted for by the addition of a mean field term[4,69] to eq 1. The equation for the susceptibility will then have the form of eq 2, where $J'$ is the interdimer coupling constant and $z$ is the number of interacting neighbors.

$$\chi'_M = \chi_M/[1 - (4zJ'/Ng^2\mu_B{}^2)\chi_M] \quad (2)$$

Magnetic data were least-squares-fitted to this equation (solid lines in Figure 9), with the $g$ value fixed at 2.16 (obtained from the Curie constant), yielding $2J = -5.70(2)$ cm$^{-1}$, $zJ' = 0.07$ cm$^{-1}$, and the agreement factor $R = 3.5 \times 10^{-5}$. These results ($J'/J \sim 0.01$) are consistent with the above description, i.e., the consideration of "quasi" isolated [$N_2OCu(\mu\text{-}C_2O_4)CuN_2O$] dimeric units with weak antiferromagnetic interactions propagated through the oxalato bridge.

## Discussion

The magnetic study of compound **1** indicates that the copper(II) ions may be viewed as essentially magnetically noncoupled. In any case, very small values of $|2J|$ would be expected since the potential pathways involving hydrogen bonds—through water molecules—offer a very poor support for the superexchange interactions. According to Coffman and Buettner,[70] $|2J|$ values less than $10^{-2}-10^{-3}$ cm$^{-1}$ ($R > 12$ Å) would be expected for compound **1**. In addition, this extended pathway implies axial positions, i.e., out-of-plane electron density. Therefore, the overlap integral is expected to be close to zero, affording a magnetically diluted system.

As it is well-known, the coordinating behavior of the oxalato anion besides the plasticity of the copper(II) ions affords a wide variety of polynuclear copper(II) complexes with oxalato as bridging ligand.[73,74] It has been previously described that compounds **3** and **5**, even though they are of different structural nature (dimeric and polymeric, respectively), can be considered as consisting in magnetically isolated $\mu$-oxalato-bridged dimers, with different topology of the framework oxalato bridge. In particular, for such dimeric systems, three limiting structures[1,52] can be depicted. We show them as A, B, and C in Chart 1.

The more remarkable differences between them refer to the relative orientation of the equatorial planes of the metal atom coordination polyhedron with regard to the oxalato plane. For structure A, with the oxalato anion occupying two basal positions, they are coplanar. On the contrary, for B and C, where the oxalato-bridge is occupying axial and equatorial coordination sites (in short, "axial−equatorial" dimers), the above-mentioned planes are perpendicular.

With regard to the magnetic properties of the dinuclear copper(II) systems, it has been shown[75−77] that the antiferromagnetic contribution $J_{AF}$ to the exchange interaction may be expressed as

$$J_{AF} = -2S(\Delta^2 - \delta^2)^{1/2} \quad (3)$$

where $S$ is the overlap integral between the magnetic orbitals centered on the two metal atoms, $\Delta$ the energy separation between the two singly occupied molecular orbitals in the triplet state built from the magnetic orbitals and $\delta$ the energy separation between the two magnetic orbitals. On the other hand, the analysis of the magnetic orbitals in $\mu$-oxalato-bridged copper(II) dimers—assuming that the magnitude of the exchange coupling is essentially governed by the square of the overlap between the magnetic orbitals—leads, for the ideal structures A, B, and C, to establish $J_B \approx 4J_A/9$ and $J_C = 0$.[50]

The great majority of the $\mu$-oxalato-bridged copper(II) dimers that have been characterized structurally belong to the structural type A. In all cases, the central [$Cu(\mu\text{-}C_2O_4)Cu$] core exhibits slight but significant deviation from planarity—the hinging $\gamma$ angle varies from 3.2° to 16.8°—with the copper atom in a more or less distorted *4+1* or *4+1+1* environment.[49,53,57] In such a topology, the unpaired electron is described as occupying $d_{x^2-y^2}$ orbital pointing from the metal toward the four nearest neighbors in an antibonding fashion. As is well-known, this coordination geometry would be advantageous to give strong antiferromag-

(72) Myers, B. E.; Berger, L.; Friedberg, S. A. *J. Appl. Phys.* **1969**, *40*, 1149.
(73) Alvarez, S.; Julve, M.; Verdaguer, M. *Inorg. Chem.* **1990**, *29*, 4500.
(74) Kitagawa, S.; Okubo, T.; Kawata, S.; Kondo, M.; Katada, M.; Kobayashi, H. *Inorg. Chem.* **1995**, *34*, 4790 and references therein.
(75) Kahn, O.; Briat, B. *J. Chem. Soc., Faraday Trans. II* **1976**, *72*, 268.
(76) Gired, J.-J.; Charlot, M. F.; Kahn, O. *Mol. Phys.* **1977**, *34*, 1063.
(77) Tola, P.; Kahn, O.; Chauvel, C.; Coudanne, H. *Nouv. J. Chim.* **1977**, *1*, 467.

**Table 4.** Structural and Magnetic Parameters for *Axial*−*Equatorial* $[XN_2Cu(\mu\text{-}C_2O_4)CuN_2X]$ Dimers (X = N, O)

| compound[a] | $2J/cm^{-1}$ | Cu−Cu/Å | $Cu-O_{ax}$/Å | $Cu-O_{eq}$/Å | $e_3$/deg | ref |
|---|---|---|---|---|---|---|
| $[\{Cu(Et_5dien)\}_2(\mu\text{-}C_2O_4)](BPh_4)_2$ | −74.8 | 5.410(1) | 2.174(4) | 1.972(4) | 42.9 | 52 |
| $[\{Cu(dien)\}_2(\mu\text{-}C_2O_4)](ClO_4)_2$ | ≈0 | 5.488(2) | 2.29(1)/2.23(1) | 2.02(1)/1.97(1) | 11.9/16.8 | 50,80 |
| $[\{Cu(tmen)(2\text{-}MeIm)\}_2(\mu\text{-}C_2O_4)](PF_6)_2$ | −13.8 | 5.434(2) | 2.208(2) | 1.997(2) | 30.2 | 50 |
| $[\{Cu(Et_5dien)\}_2(\mu\text{-}C_2O_4)](PF_6)$ | −19.2 | 5.457(2) | 2.229(2) | 1.971(4) | 27.5 | 52,81 |
| $[\{Cu(BIP)\}_2(\mu\text{-}C_2O_4)]\cdot 6H_2O$ | −5.7 | 5.52(1) | 2.266(3) | 2.001(3) | 26.2 | this work |

[a] $Et_5$dien = *N,N,N′,N″,N″*-pentamethylethylenetriamine, dien = diethylenetriamine, 2-MeIm = 2-methylimidazole, tmen = *N,N,N′,N′*-tetramethylethylenediamine.

netic interactions through the multi-atom bridge, since the magnitude of the antiferromagnetic contribution ($J_{AF}$) is essentially governed by their delocalization onto the oxygen atoms of the oxalato bridge, which constitutes an excellent support for the exchange.[73,78] The reported values of the singlet−triplet gap (−2*J*) for these systems, vary approximately from 300 to 400 $cm^{-1}$ for those with centrosymmetric $[Cu(\mu\text{-}C_2O_4)Cu]$ core[53,57,73] and from 260 to 300 $cm^{-1}$ for those with noncentrosymmetric core.[49,53] The significant weakening of the interaction of the noncentrosymmetric dimers with regard to the centrosymmetric ones may be attributed to the lowering of symmetry, with $\delta \neq 0$ for the latter and the corresponding decreasing of the antiferromagnetic contribution ($J_{AF}$ in eq 3).[3,77] Although the *J* values are only slightly sensitive to changes in significant structural parameters, several attempts have been performed to analyze the more relevant features in order to explore the existence of magneto-structural correlations. One of these features to be highlighted is the correlation reported by Alvarez et al.[73] between the magnitude of the antiferromagnetic interaction and the bending angle $\gamma$ in the $[Cu(\mu\text{-}C_2O_4)Cu]$ core: the absolute value of $|2J|$ decreasing as $\gamma$ increases. This suggested correlation works for those dimers having terminal ligands of relative low basicity as bipyridine or phenantroline, but significant deviation for several compounds with other terminal ligands is observed. A variety of factors influencing the value of 2*J* in dinuclear complexes must be considered to explain this, such as, the metal−metal separation, the dihedral angle between the planes containing the magnetic orbitals, the metal-bridge ligand bond and angles, the metal ion stereochemistry, the terminal ligand basicity, etc.

The absolute $|2J|$ value obtained for compound **3** (265 $cm^{-1}$) is significantly smaller that those observed in analogous centrosymmetric $\{XN_2Cu(\mu\text{-}C_2O_4)CuN_2X\}$ dimers and similar to that evaluated for noncentrosymmetric ones. Nevertheless, all topological parameters for both the $[Cu(\mu\text{-}C_2O_4)Cu]$ core and the $CuN_2O_2Cl$ chromophore fall in the range of those reported for analogous compounds, and the basicity of the HBIP can be estimated to be close to the mean value of the usual terminal ligands. Hence, the interpretation of the comparatively low value of 2*J* obtained for compound **3**, remains as an open question. It has been recently[79] reported an alternating $\mu$-azido-$\mu$-oxalato chain which, despite its polymeric nature, can be considered as consisting of magnetically isolated centrosymmetric $[Cu(\mu\text{-}C_2O_4)Cu]$ units. A relatively "low" value of 2*J* (−287 $cm^{-1}$) has been evaluated for the dimeric fragments, but no interpretation has been suggested.

The most relevant data for the structural and magnetically characterized axial−equatorial $\mu$-oxalato-bridged copper(II) dimers with five-coordinated terminal copper atoms are summarized in Table 4. The coordination around the copper(II) ions varies between the two ideal geometries, TBP (B-type) and SP (C-type), the extent of the exchange interaction being significantly affected by the stereochemistry of the metal atoms. The key shape-determining angle $e_3$ (see crystal structure description) can be used in order to parametrize the distortion of the coordination polyhedron. From Table 4, it should be stressed that the weakest interactions are found for the complexes with nearly SP copper(II) coordination geometry, while the interaction becomes stronger as the predominance of the TBP character increases.[50,52] In these systems the exchange is essentially propagated by through-space O−O interaction in the COO fragments of the oxalato group. Taking into account that the present interaction is predominantly axial−equatorial, the progressive increase of the $z^2$-type character acquired by the magnetic orbitals in the distortion of the SP stereochemistry enhances the overlap between the magnetic orbitals via the COO units.[1,4,52] If the 2*J* values are plotted vs the $e_3$ angle (Figure 10), a rough correlation emerges between the exchange coupling and the distortion of the pentacoordinated copper(II) geometry: the magnetic coupling becomes less antiferromagnetic as the $e_3$ angle diminishes, and it seems to become negligible for ca. $e_3 < 15°$. From the outlined correlation a 2*J* value of ca −160 $cm^{-1}$ could be tentatively predicted for limiting TBP geometry. Assuming that the mean of $|2J_A|$ for centrosymmetric dimers is ca. 350 ± 50 $cm^{-1}$, and that $|2J_B|$ is expected to be close to $4/9|2J_A|$ (see above), a value of ca. 160 ± 20 $cm^{-1}$ might be derived for the dimers with type B structure. Thus, despite the substantial simplifications introduced, the sketched correlation are in acceptable agreement with the theoretical considerations and support that in axial−equatorial $\mu$-oxalato copper(II) dimers, the stereochemistry of the metal atoms exert a remarkable influence on the exchange interaction, which is governed by the magnitude of the overlap between the magnetic orbitals. On the other hand, other outstanding structural parameters as, for instance, the Cu−Cu and Cu−O(oxalato) distances, do not correlate with the copper(II)−copper(II) interaction. The number

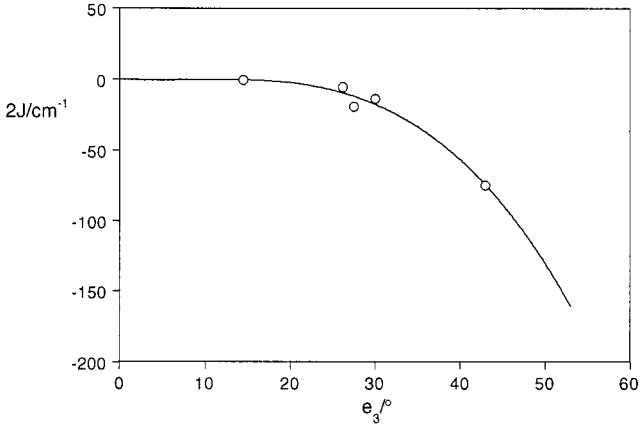


**Figure 10.** Variation of the *2J* parameter vs $e_3$ angle (see text) for axial−equatorial $[XN_2Cu(\mu\text{-}C_2O_4)CuN_2X]$ dimers (X = N,O).

(78) Kahn, O. *Angewt. Chem., Int. Ed. Engl.* **1985**, *24*, 834.
(79) Vicente, R.; Escuer, A.; Ferretjans, J.; Stoeckli-Evans, H.; Solans, X.; Font-Bardía, M. *J. Chem. Soc., Dalton Trans.* **1997**, 167.
(80) Curtis, N. F.; McCormick, I. R. N.; Waters, T. N. *J. Chem. Soc., Dalton Trans.* **1973**, 1537.
(81) Sletten, J. *Acta Chem. Scand., Ser. A* **1983**, *A37*, 569.

of axial−equatorial dimers with $\{XN_2Cu(\mu\text{-}C_2O_4)CuN_2X\}$ cores characterized magnetic and structurally is relatively scarce, and further data are necessary in order to study in depth the magneto-structural correlations in such systems.

Finally, with regard to compound **4**, some considerations can be outlined. The IR study suggests the presence of bis-bidentate oxalato groups as well as mono-coordinated carboxylate groups. Thus, a molecular structure could be proposed for compound **4** related to that observed for compound **5** (see structural part) with $\mu$-oxalato dimeric fragments $[Cu(\mu\text{-}C_2O_4)Cu]$ as the prevalent responsibles of the interaction. Obviously, the lack of structural data precludes any accurate analysis of the observed behavior, but the high value of $|2J|$ compared with that observed in compound **5**, might indicate substantial differences in both the metal atom environment and the central $[Cu(\mu\text{-}C_2O_4)Cu]$ core. The bridging network most probably present in compound **4** can be expected to be intermediate between the ideal geometries A and B, in agreement with the vibrational and electronic spectra.

**Acknowledgment.** We are grateful to the DGICYT (PB93-0688) for financial support. We thank Drs A. Mari and F. Lloret for their assistance with the magnetic measurements.

**Supporting Information Available:** Tables listing detailed crystallographic data, atomic positional parameters, anisotropic thermal parameters, bond lengths and angles, and least-squares planes are available free of charge via the Internet at http://pubs.acs.org.

IC980982X